Published for SISSA by Springer

Received: *March 26, 2020*
Accepted: *April 22, 2020*
Published: *May 20, 2020*

Sgoldstino signature in hh, W^+W^- and ZZ spectra at the LHC

S. Demidov,[a,b] **D. Gorbunov**[a,b] **and E. Kriukova**[a,c]

[a] *Institute for Nuclear Research of the Russian Academy of Sciences, 60th October Anniversary prospect 7a, Moscow 117312, Russia*
[b] *Moscow Institute of Physics and Technology, Institutsky per. 9, Dolgoprudny 141700, Russia*
[c] *Department of Physics, Lomonosov Moscow State University, Leninskie Gory, Moscow 119991, Russia*

E-mail: demidov@inr.ac.ru, gorby@inr.ac.ru, kryukova.ea15@physics.msu.ru

Abstract: In a supersymmetric extension of the Standard Model of particle physics (SM) with low scale of supersymmetry breaking, sgoldstino of (sub)TeV mass can be observed at the Large Hadron Collider (LHC) as a peak in diboson mass spectra. Moreover, as a singlet with respect to the SM gauge group, scalar sgoldstino can mix with the SM-like Higgs boson and interfere in all neutral channels providing with the promising signatures of new physics if superpartners are heavy. Sgoldstino couplings to the SM particles are determined by the pattern of soft supersymmetry breaking parameters. Here we concentrate on the cases with a noticeable sgoldstino contribution to di-Higgs channel. Having found a phenomenologically viable region in the model parameter space where scalar sgoldstino, produced at the LHC in gluon fusion, decays into a pair of the lightest Higgs boson we give predictions for corresponding cross section. Using the results of the LHC searches for scalar resonances we place bounds on the supersymmetry breaking scale $\sqrt{F}$ in this region of parameter space. Remarkably, in this region sgoldstino may also be observed in W^+W^- and ZZ channels, yielding independent signatures, since their signal strengths are related to that of di-Higgs channel.

Keywords: Supersymmetry Phenomenology

ArXiv ePrint: 2003.07388

https://doi.org/10.1007/JHEP05(2020)092

JHEP05(2020)092

Contents

1 Introduction 1

2 The model 2

3 Sgoldstino production and decay channels 8
- 3.1 Production of scalar sgoldstino 8
- 3.2 Sgoldstino decays 10

4 Phenomenology of the resonant sgoldstino signature 15

5 Conclusions 19

A Trilinear coefficients for a set of sgoldstino-Higgs bosons vertices 21

B Trilinear coefficients in the mass basis for a set of sgoldstino-Higgs bosons vertices 21

JHEP05(2020)092

1 Introduction

The first stages of LHC running culminated in 2012 with the discovery of the Higgs boson [1, 2]. Further experimental program of the LHC experiments includes measurement and precise determination of the Higgs boson coupling constants using data on the Higgs boson production cross sections and decay widths. Numerous models of new physics predict deviations of these coupling constants from their SM values. In this respect, the Higgs boson self-coupling is of great interest as several classes of SM extensions imply some modification of the Higgs sector. Double Higgs boson production is one of the most sensitive observables to the Higgs boson self-interaction and specific modifications of the Higgs sector. This process is expected to be seen with various signatures at LHC (see ref. [3] for a review) operating in the high luminosity regime (HL-LHC). A deviation of the cross section from the SM prediction could indicate possible ways to extend the SM.

The cross section of the di-Higgs production in proton collisions in the SM was calculated in [4–9]. The double Higgs boson production can be resonantly enhanced if the Higgs sector contains new scalar(s) with the mass around TeV scale. Examples of such scenarios were discussed in refs. [10–16]. In this paper we consider supersymmetric models with low scale supersymmetry breaking (see e.g. [17–25]). In this class of models the lightest supersymmetric particle is gravitino which acquires its mass via the super-Higgs mechanism [26–28]. The longitudinal component of gravitino appears after spontaneous supersymmetry breaking as a derivative of the Goldstone fermion — goldstino G. The latter can be the fermionic component of a chiral supermultiplet,

$$\Phi = \phi + \sqrt{2}\theta G + \theta^2 F_\phi \,, \tag{1.1}$$

where θ is the Grassmannian coordinate, ϕ is the complex scalar field called sgoldstino and F_ϕ is the auxiliary field which acquires non-zero vev, i.e. $\langle F_\phi \rangle = F$, triggering spontaneous SUSY breaking in the entire model. Here we consider scenarios in which the scale $\sqrt{F}$ of SUSY breaking is not very far from the electroweak scale while all the fields in the hidden sector except for those belonging to the goldstino multiplet are heavy. The purpose of our study is to investigate possibility of the resonant enhancement of di-Higgs production at the LHC due to contribution of relatively light scalar sgoldstino. To make the picture as clear as possible, yet realistic and phenomenologically viable, we restrict ourselves to the case in which all superpartners of the SM particles are also relatively heavy.

Though model-dependent, but typically the main sgoldstino production mechanism in pp collisions is through gluon-gluon fusion [29]. Being even with respect to R-parity, sgoldstino can decay into pairs of the SM particles. We single out the part of the parameter space where branching fraction of sgoldstino decay into pair of the Higgs bosons is close to the largest possible value which is 25%. This region of the model parameter space corresponds to sufficiently large mixing between sgoldstino and the lightest Higgs boson which can result in an amplification of the corresponding decay width and consequently di-Higgs production cross section. In this regime sgoldstino decays dominantly into hh, W^+W^- and ZZ with partial widths related as 1:2:1 respectively. We discuss the sgoldstino signature in spectra of these final states at the LHC and calculate cross sections of the corresponding processes. Using present experimental constraints on production of the scalar resonances decaying into the heavy bosons we obtain bounds on the SUSY breaking scale.

This paper is organized as follows. In section 2 we describe the model Lagrangian and derive the potential of scalar fields. We discuss interaction of sgoldstino and Higgs bosons and mixing in this sector. We obtain sgoldstino-Higgs bosons trilinear couplings. The scalar sgoldstino production channels and decay modes are discussed in section 3. There we outline a region in the model parameter space where sgoldstino can decay into pair of the lightest Higgs bosons as well as into the pair of the massive vector bosons with a considerable probabilities. The resonant behavior of the di-Higgs, W^+W^- and ZZ cross sections and their dependence on model parameters are investigated in section 4. There we also present bounds on the supersymmetry breaking scale extracted from results of ATLAS and CMS experiments in searches for di-boson resonances. Our findings are summarized in section 5. Appendices are reserved for explicit expressions for trilinear coupling constants of the neutral scalars.

2 The model

We consider a supersymmetric extension of the Standard Model with the chiral goldstino superfield (1.1). The model includes the Minimal Supersymmetric Standard Model (MSSM) in which soft supersymmetry breaking terms are generated through interactions with Φ, when the auxiliary component of F_Φ gets replaced with its non-zero vacuum expectation value, i.e. $\langle F_\phi \rangle = F$. The Lagrangian of the model can be written (see e.g. [30]) as the sum

$$\mathcal{L} = \mathcal{L}_K + \mathcal{L}_W + \mathcal{L}_{\text{gauge}} + \mathcal{L}_\Phi \tag{2.1}$$

JHEP05(2020)092

of the contributions from the Kähler potential $\mathcal{L}_K$, superpotential $\mathcal{L}_W$, vector fields $\mathcal{L}_{\text{gauge}}$ and a part which describes dynamics of the goldstino supermultiplet $\mathcal{L}_\Phi$. The first term in (2.1) has the form

$$\mathcal{L}_K = \int d^2\theta d^2\bar{\theta} \sum_k \left(1 - \frac{m_k^2}{F^2}\Phi^\dagger\Phi\right) \Phi_k^\dagger e^{g_1 V_1 + g_2 V_2 + g_3 V_3} \Phi_k, \tag{2.2}$$

where the sum is taken over all matter superfields Φ_k. The parts $\mathcal{L}_W$ and $\mathcal{L}_{\text{gauge}}$ read

$$\begin{aligned}\mathcal{L}_W = \int d^2\theta \epsilon_{ij} \Bigg(&\left(\mu - \frac{B}{F}\Phi\right) H_D^i H_U^j + \left(Y_{ab}^L + \frac{A_{ab}^L}{F}\Phi\right) L_a^j E_b^c H_D^i + \\ &+ \left(Y_{ab}^D + \frac{A_{ab}^D}{F}\Phi\right) Q_a^j D_b^c H_D^i + \left(Y_{ab}^U + \frac{A_{ab}^U}{F}\Phi\right) Q_a^i U_b^c H_U^j \Bigg) + h.c.,\end{aligned} \tag{2.3}$$

and

$$\mathcal{L}_{\text{gauge}} = \frac{1}{4}\sum_a \int d^2\theta \left(1 + \frac{2M_a}{F}\Phi\right) \text{Tr} W_\alpha W^\alpha + h.c.\,, \tag{2.4}$$

where sum goes over $a = 3, 2, 1$, correspondingly to all the SM gauge groups $\text{SU}(3)_c$, $\text{SU}(2)_w$, $\text{U}(1)_Y$. Here μ is the higgsino mixing parameter, L, E are the left and right lepton superfields, Q, U, D are the superfields of left, right up and right down quarks, respectively, H_U, H_D are two Higgs doublet superfields, $Y^{L,D,U}$ are the matrices of the Yukawa coupling constants. The interactions of Φ with other matter fields of MSSM, which yield soft terms after SUSY breaking with the parameters m_k^2, M_a, B, $A_{ab}^{L,D,U}$, are suppressed by F. The dynamics of goldstino supermultiplet is modeled by the Lagrangian

$$\mathcal{L}_\Phi = \int d^2\theta d^2\bar{\theta} \left(\Phi^\dagger\Phi - \frac{m_s^2+m_p^2}{8F^2}(\Phi^\dagger\Phi)^2 - \frac{m_s^2-m_p^2}{12F^2}(\Phi^\dagger\Phi^3 + \Phi^{\dagger 3}\Phi)\right) - \left(\int d^2\theta F\Phi + h.c.\right), \tag{2.5}$$

where m_s^2 and m_p^2 are mass parameters for scalar and pseudoscalar sgoldstino fields. The model described above should be considered as an effective theory which contains higher order interaction terms suppressed by higher powers of F and for consistency we require smallness of the soft parameters, $m_{soft} \ll \sqrt{F}$.

Using the Lagrangian (2.1) one can obtain the scalar potential of the Higgs and sgoldstino sector (see also [31])

$$V = V_{11} + V_{12} + V_{21} + V_{22}, \tag{2.6}$$

$$V_{11} = \frac{g_1^2}{8}\left(1 + \frac{M_1}{F}(\phi + \phi^*)\right)^{-1} \left[h_d^\dagger h_d - h_u^\dagger h_u - \frac{\phi^*\phi}{F^2}\left(m_d^2 h_d^\dagger h_d - m_u^2 h_u^\dagger h_u\right)\right]^2, \tag{2.7}$$

$$V_{12} = \frac{g_2^2}{8}\left(1 + \frac{M_2}{F}(\phi + \phi^*)\right)^{-1} \left[h_d^\dagger \sigma_a h_d + h_u^\dagger \sigma_a h_u - \frac{\phi^*\phi}{F^2}\left(m_d^2 h_d^\dagger \sigma_a h_d + m_u^2 h_u^\dagger \sigma_a h_u\right)\right]^2. \tag{2.8}$$

$$\begin{aligned}V_{21} = \Bigg(1 - \frac{m_s^2+m_p^2}{2F^2}\phi^*\phi - \frac{m_s^2-m_p^2}{4F^2}\left(\phi^2 + \phi^{*2}\right) - \frac{m_u^2}{F^2}h_u^\dagger h_u - \frac{m_d^2}{F^2}h_d^\dagger h_d - \frac{m_u^4}{F^4}\phi^*\phi h_u^\dagger h_u - \\ - \frac{m_d^4}{F^4}\phi^*\phi h_d^\dagger h_d\Bigg)^{-1} \left|F + \left(-h_d^0 h_u^0 + H^- H^+\right)\left(\frac{B}{F} - \frac{m_u^2+m_d^2}{F^2}\phi^*\left(\mu - \frac{B}{F}\phi\right)\right)\right|^2,\end{aligned} \tag{2.9}$$

$$V_{22} = \frac{\mu^2}{F^2}|\phi|^2\left(m_u^2 h_d^\dagger h_d + m_d^2 h_u^\dagger h_u\right) + \left|\mu - \frac{B}{F}\phi\right|^2\left(h_d^\dagger h_d + h_u^\dagger h_u\right). \tag{2.10}$$

JHEP05(2020)092

Here $h_d = \left(h_d^0, H^-\right)^T$, $h_u = \left(H^+, h_u^0\right)^T$ are the Higgs doublets and we consider pall the parameters entering the potential to be real. As $\sqrt{F}$ is the largest scale in the model, we are interested in the scalar potential to the leading order in $1/F$. Moreover, since each sgoldstino field enters the interaction terms with factor $1/F$, rates of multi-sgoldstino processes are naturally parametrically suppressed. Therefore, the most promising processes are those involving single sgoldstino production.

Now we expand the scalar fields around their vacuum expectation values. For the Higgs fields we have, as usual [32]

$$h_u^0 = v_u + \frac{1}{\sqrt{2}}(h\cos\alpha + H\sin\alpha) + \frac{i}{\sqrt{2}}A\cos\beta, \tag{2.11}$$

$$h_d^0 = v_d + \frac{1}{\sqrt{2}}(-h\sin\alpha + H\cos\alpha) + \frac{i}{\sqrt{2}}A\sin\beta\,, \tag{2.12}$$

where $v_u \equiv v\sin\beta$, $v_d \equiv v\cos\beta$, $v = 174\,\text{GeV}$. Sgoldstino field is expanded as

$$\phi = \frac{1}{\sqrt{2}}(s + ip)\,, \tag{2.13}$$

where s and p are its scalar and pseudoscalar components. In general, the sgoldstino field acquires a non-zero vev $\langle\phi\rangle = v_\phi$ and one can show [33] that v_ϕ scales as $1/F$ for scalar sgoldstino heavier than the lightest Higgs boson. Therefore, the terms with sgoldstino vev would contribute to the terms with smaller number of sgoldstino fields but suppressed by powers of $1/F^2$ and hence are neglected in what follows. Naturally, for consistency reasons, we set $v_\phi = 0$. Likewise, point $h_u^0 = v_u$, $h_d^0 = v_d$ is a true vacuum up to corrections suppressed by powers of $1/F^2$, which we ignore.[1]

One can substitute the expansions (2.11)–(2.13) into the potential (2.7)–(2.10) and find the sgoldstino-Higgs boson vertices to the leading order in $1/F$. In order to simplify expressions for the interaction terms, let us introduce the notations

$$m_Z^2 \equiv \frac{g_1^2 + g_2^2}{2}v^2, \qquad m_A^2 \equiv m_u^2 + m_d^2 + 2\mu^2\,, \tag{2.14}$$

which correspond to tree-level squared masses of Z-boson and Higgs pseudoscalar A. For the true vacuum there are no terms linear in h, H in the potential, and so no linear terms within our approximation. Minimization of the scalar potential results in the following relationships [32]

$$\frac{1}{2}m_Z^2 + \mu^2 = \frac{m_d^2 - m_u^2\tan^2\beta}{\tan^2\beta - 1}, \tag{2.15}$$

$$\sin 2\beta = \frac{2B}{m_A^2}. \tag{2.16}$$

The mixing angle α in eqs. (2.11) and (2.12) is chosen in the standard way [32]

$$\frac{\tan 2\alpha}{\tan 2\beta} = \frac{m_A^2 + m_Z^2}{m_A^2 - m_Z^2}. \tag{2.17}$$

[1] Let us note that for $\sqrt{F} \sim$ few TeV the corrections of order $1/F^2$ to the scalar potential can be valuable and contribute considerably to the mass of the lightest Higgs boson [34]. For the choice of parameters considered in the present study these corrections are negligible.

JHEP05(2020)092

Once again, any possible corrections suppressed by powers of $1/F^2$ are small and neglected here. At the same time the loop corrections to the effective potential should be large enough to generate observed value of the Higgs boson mass. Their size is determined mainly by interactions with top-stop sector. In what follows we do not discuss squark sector of the model and just assume squarks to be sufficiently heavy. Therefore, we treat the quantum corrections which contribute to the Higgs boson masses as obligatory and of the size sufficient for saturating the lightest Higgs boson mass. Consequently, we neglect radiative corrections to the mixing term between h and H, that is justified by the decoupling regime we assume in this study.

The mass terms in the Lagrangian for the scalar (H, h, s) and pseudoscalar (A, p) fields have the following matrix form

$$\frac{1}{2}\begin{pmatrix} H & h & s \end{pmatrix}\begin{pmatrix} m_H^2 & 0 & Y/F \\ 0 & m_h^2 & X/F \\ Y/F & X/F & m_s^2 \end{pmatrix}\begin{pmatrix} H \\ h \\ s \end{pmatrix} + \frac{1}{2}\begin{pmatrix} A & p \end{pmatrix}\begin{pmatrix} m_A^2 & Z/F \\ Z/F & m_p^2 \end{pmatrix}\begin{pmatrix} A \\ p \end{pmatrix}, \tag{2.18}$$

where the mixing terms read

$$X \equiv v\Bigg(\frac{g_1^2 M_1 + g_2^2 M_2}{2} v^2 \cos 2\beta \sin(\alpha+\beta) + \\ + \mu m_A^2 \sin 2\beta \sin(\alpha-\beta) + \left(m_A^2 - 2\mu^2\right)\mu \cos(\alpha+\beta)\Bigg), \tag{2.19}$$

$$Y \equiv -v\Bigg(\frac{g_1^2 M_1 + g_2^2 M_2}{2} v^2 \cos 2\beta \cos(\alpha+\beta) + \\ + \mu m_A^2 \sin 2\beta \cos(\alpha-\beta) + \left(2\mu^2 - m_A^2\right)\mu \sin(\alpha+\beta)\Bigg), \tag{2.20}$$

$$Z \equiv \mu v\left(m_A^2 - 2\mu^2\right). \tag{2.21}$$

According to the above discussion the diagonal values of the mass matrices, i.e. m_h^2, m_H^2 and m_A^2 already contain leading quantum corrections. Recall, that our primary goal is to consider the possible sgoldstino contribution to the pair productions of the lightest Higgs bosons h which are interpreted as the scalar Higgs-like particles discovered at the LHC. We present below expressions for the relevant trilinear coupling constants in the scalar sector. Corresponding part of the interaction Lagrangian is

$$\mathcal{L}_{\text{trilinear}} = C_{hhh}h^3 + C_{hhH}h^2 H + C_{hHH}hH^2 + C_{HHH}H^3 + C_{shh}sh^2 + C_{sHH}sH^2, \tag{2.22}$$

where

$$C_{hhh} \equiv \frac{1}{2\sqrt{2}}\frac{m_Z^2}{v}\cos 2\alpha \sin(\alpha+\beta), \tag{2.23}$$

$$C_{HHH} \equiv \frac{1}{2\sqrt{2}}\frac{m_Z^2}{v}\cos 2\alpha \cos(\alpha+\beta), \tag{2.24}$$

$$C_{hhH} \equiv \frac{1}{4\sqrt{2}}\frac{m_Z^2}{v}\left(\cos(\alpha-\beta) - 3\cos(3\alpha+\beta)\right), \tag{2.25}$$

$$C_{hHH} \equiv -\frac{1}{4\sqrt{2}}\frac{m_Z^2}{v}\left(\sin(\alpha-\beta) + 3\sin(3\alpha+\beta)\right) \tag{2.26}$$

JHEP05(2020)092

are the MSSM Higgs trilinear couplings and

$$C_{sHH} \equiv \frac{1}{F\sqrt{2}}\left(-\frac{v^2}{4}\left(g_1^2 M_1 + g_2^2 M_2\right)\left(2\cos 2\alpha \cos 2\beta - \sin 2\alpha \sin 2\beta + 1\right) + \right.$$
$$\left. + \mu \sin 2\alpha \left[\frac{m_A^2}{2}\left(1 - \frac{\sin 2\beta}{\sin 2\alpha}\right) - \mu^2\right]\right). \tag{2.27}$$

$$C_{shh} \equiv \frac{1}{F\sqrt{2}}\left(\frac{v^2}{4}\left(g_1^2 M_1 + g_2^2 M_2\right)\left(2\cos 2\alpha \cos 2\beta - \sin 2\alpha \sin 2\beta - 1\right) - \right.$$
$$\left. - \mu \sin 2\alpha \left[\frac{m_A^2}{2}\left(1 + \frac{\sin 2\beta}{\sin 2\alpha}\right) - \mu^2\right]\right) \tag{2.28}$$

are the trilinear coupling constants of the interaction between scalar sgoldstino and the Higgs bosons. Other trilinear couplings in the scalar sector are not relevant for the di-Higgs boson production in the model to the leading order in $1/F$. However, in appendix A we present expressions for those interaction terms containing single sgoldstino and two Higgs bosons for completeness. They agree with the similar expressions in refs. [31, 35].

At $F \to \infty$ the decompositions (2.11), (2.12) and (2.13) make the mass matrices of the component fields (H, h, s) and (A, p) diagonal at tree level. At finite F and relatively light sgoldstino considered in this study the mixing between these fields can result in a considerable modification of the model phenomenology. Being interested primary in hh final state we concentrate below on the mixing in the scalar sector, i.e. between H, h and s, and denote the mass states as $\tilde{H}$, $\tilde{h}$ and $\tilde{s}$. Similar transformation can be also performed for the mass matrix of pseudoscalars A, p by introducing fields $\tilde{A}, \tilde{p}$.

In order to make the 3×3 mass squared matrix in eq. (2.18) diagonal, we consider the following rotation which is parameterized by the mixing angles ϕ, ψ, θ

$$\begin{pmatrix} \cos\phi & \sin\phi & 0 \\ -\sin\phi & \cos\phi & 0 \\ 0 & 0 & 1 \end{pmatrix}\begin{pmatrix} \cos\psi & 0 & \sin\psi \\ 0 & 1 & 0 \\ -\sin\psi & 0 & \cos\psi \end{pmatrix}\begin{pmatrix} 1 & 0 & 0 \\ 0 & \cos\theta & \sin\theta \\ 0 & -\sin\theta & \cos\theta \end{pmatrix} \times$$
$$\times \begin{pmatrix} m_H^2 & 0 & Y/F \\ 0 & m_h^2 & X/F \\ Y/F & X/F & m_s^2 \end{pmatrix} \times$$
$$\times \begin{pmatrix} 1 & 0 & 0 \\ 0 & \cos\theta & -\sin\theta \\ 0 & \sin\theta & \cos\theta \end{pmatrix}\begin{pmatrix} \cos\psi & 0 & -\sin\psi \\ 0 & 1 & 0 \\ \sin\psi & 0 & \cos\psi \end{pmatrix}\begin{pmatrix} \cos\phi & -\sin\phi & 0 \\ \sin\phi & \cos\phi & 0 \\ 0 & 0 & 1 \end{pmatrix}. \tag{2.29}$$

Hereinafter we work in the approximation of the small mixing angles. Given that the mixing terms are suppressed by $1/F$ we take the angles ϕ, ψ, θ to the leading non-zero order in $1/F$. Then by writing the condition of zero off-diagonal elements in the first-order approximation in (2.29) one can obtain the expressions for the mixing angles

$$\psi = \frac{Y}{F(m_H^2 - m_s^2)}, \tag{2.30}$$

$$\theta = \frac{X}{F(m_h^2 - m_s^2)}, \tag{2.31}$$

JHEP05(2020)092

while as 1-2 and 2-1 elements in the mass matrix (2.18) are equal to zero, the third mixing angle ϕ appears to be of the second order in $1/F$:

$$\phi = \frac{XY}{F^2(m_h^2 - m_s^2)(m_H^2 - m_h^2)}\,. \tag{2.32}$$

It can be easily seen from the equations (2.30), (2.31), (2.32) that the mixing angles ψ, θ, ϕ can be quite large if the corresponding masses m_h, m_H, m_s are close to each other. In what follows we do not consider the case of degenerate scalars to avoid large values of the mixing angles (that pattern may be unrealistic in any cases given measurements at the LHC).

Rotation to the mass eigenstates denoted as $\tilde{H}$, $\tilde{h}$, $\tilde{s}$ is given by $\begin{pmatrix} H & h & s \end{pmatrix} = \begin{pmatrix} \tilde{H} & \tilde{h} & \tilde{s} \end{pmatrix} C$, where in the approximation of small mixing the rotation matrix C can be written as

$$C = \begin{pmatrix} 1 - \psi^2/2 & \phi - \psi\theta & \psi \\ -\phi & 1 - \theta^2/2 & \theta \\ -\psi & -\theta & 1 - \psi^2/2 - \theta^2/2 \end{pmatrix}. \tag{2.33}$$

Similar calculations can be performed for the mass matrix of the pseudoscalar fields. Corresponding mixing angle ξ reads

$$\xi = \frac{Z}{F(m_A^2 - m_p^2)}. \tag{2.34}$$

In the basis of mass eigenstates the trilinear coupling constants which are relevant for resonant production of the pair of the lightest Higgs bosons can be written as follows

$$\mathcal{L}_{\tilde{s}\tilde{h}\tilde{h}} = (C_{shh} - 3C_{hhh}\theta - C_{hhH}\psi)\,\tilde{s}\tilde{h}\tilde{h} \equiv C_{\tilde{s}\tilde{h}\tilde{h}}\tilde{s}\tilde{h}\tilde{h}\,, \tag{2.35}$$

where we omitted the terms of order $1/F^2$ and higher.

In the next sections these vertices are used in the calculation of sgoldstino decay rate into a pair of neutral Higgs bosons and of the resonant double-Higgs production cross section. Expressions for other vertices with one sgoldstino and two Higgs bosons ($\tilde{s}\tilde{h}\tilde{H}$, $\tilde{s}\tilde{A}\tilde{A}$, $\tilde{s}\tilde{H}^+\tilde{H}^-$, $\tilde{p}\tilde{A}\tilde{H}$, $\tilde{p}\tilde{A}\tilde{h}$), irrelevant for the present study, can be found in appendix B.

In the next sections we will discuss production and decay of scalar sgoldstino. The relevant part of the Lagrangian describing interactions of the scalar sgoldstino s with SM vector bosons has the form

$$\mathcal{L}_s^{\text{eff}} = -\frac{M_2}{\sqrt{2}F} s W^{\mu\nu *} W_{\mu\nu} - \frac{M_{ZZ}}{2\sqrt{2}F} s Z^{\mu\nu} Z_{\mu\nu} - \frac{M_{Z\gamma}}{\sqrt{2}F} s F^{\mu\nu} Z_{\mu\nu} \tag{2.36}$$

$$- \frac{M_{\gamma\gamma}}{2\sqrt{2}F} s F^{\mu\nu} F_{\mu\nu} - \frac{M_3}{2\sqrt{2}F} s\; G^{a\mu\nu} G^a_{\mu\nu}\,, \tag{2.37}$$

where $W_{\mu\nu}$, $Z_{\mu\nu}$, $F_{\mu\nu}$ and $G^a_{\mu\nu}$ are the field strength tensors for the $W^\pm$-bosons, Z-boson, photon and gluons respectively; the mass parameters in front of the couplings read

$$M_{ZZ} \equiv M_1 \sin^2\theta_W + M_2 \cos^2\theta_W, \quad M_{\gamma\gamma} \equiv M_1 \cos^2\theta_W + M_2 \sin^2\theta_W\,, \tag{2.38}$$

$$M_{Z\gamma} \equiv (M_2 - M_1)\cos\theta_W \sin\theta_W\,. \tag{2.39}$$

JHEP05(2020)092

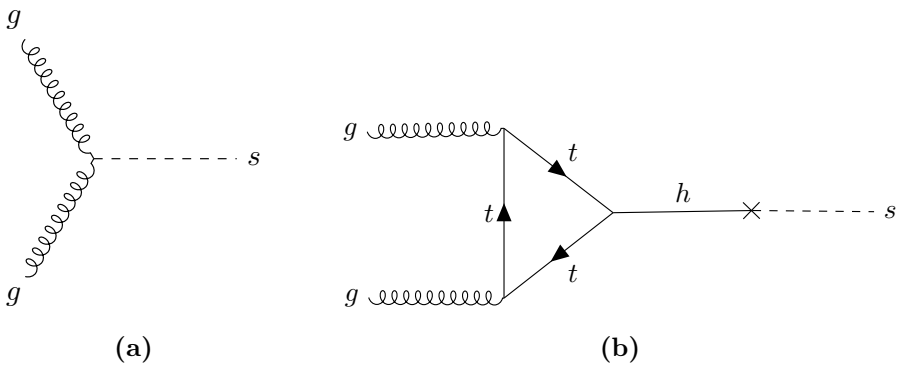

Figure 1. Feynman diagrams for the sgoldstino production via gluon fusion to the leading order in $1/F$; the cross refers to the Higgs-sgoldstino mixing.

Interactions (2.36) along with (2.22) and sgoldstino-Higgs mixing given by (2.33) determine phenomenology of TeV scale scalar sgoldstino at hadron colliders. Results of our analysis depend upon the following parameters: $\tan\beta$, μ, m_A, m_s, M_1, M_2, M_3, F. Since formulas of section 2 are obtained in the small mixing angles approximation, one should keep only those models in the parameter space that correspond to small mixing angles ψ, θ (for the numerical calculations we select the models with $\theta < 0.3$, $\psi < 0.3$).

3 Sgoldstino production and decay channels

To understand possible size of the resonant double Higgs boson production in the model we need to study sgoldstino production in proton collisions and its subsequent decay. Here we refer to refs. [29, 35–40] for previous studies of sgoldstino collider phenomenology. To simplify notations, in what follows we use s and h for the mass eigenstates (which were denoted as $\tilde{s}$ and $\tilde{h}$ in the previous section) and take into account contributions from the sgoldstino-Higgs mixing to the leading order in $1/F$.

3.1 Production of scalar sgoldstino

For typical hierarchy between the soft SUSY breaking parameters the dominant sgoldstino production mechanism is gluon fusion [29]. This process, $gg \to s$, occurs in this model already at the tree level due to sgoldstino interaction with gluons governed by the coupling M_3/F, see eq. (2.36). Mixing with the Higgs bosons yields additional contributions to the amplitude of this process, see figures 1a, 1b. The contribution from sgoldstino mixing with heavy neutral Higgs (similar to figure 1b) is suppressed by $1/\tan\beta$ from the $Ht\bar{t}$ vertex and also by square of its mass m_H^2 in the expression for the corresponding mixing angle, therefore we neglect it in the following calculation of sgoldstino production cross section. The leading order cross section of the sgoldstino production in gluon fusion can be calculated using the parton distribution function (PDF) $g(x, m_s^2)$ of gluons in proton as

$$\sigma_{\text{prod}}(pp \to s) = \sigma_0 \tau \int_\tau^1 \frac{\mathrm{d}x}{x} g\left(x, m_s^2\right) g\left(\frac{\tau}{x}, m_s^2\right), \tag{3.1}$$

JHEP05(2020)092

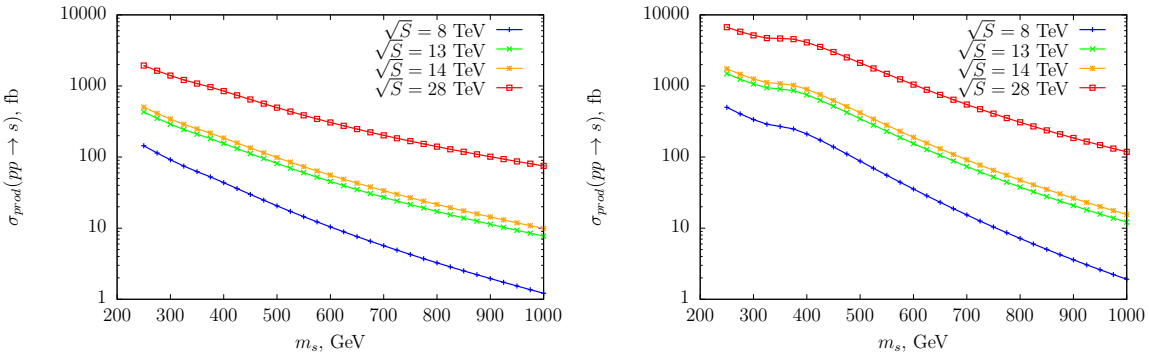

Figure 2. Sgoldstino production cross section for a set of total energies of protons $\sqrt{S}$, and model parameters fixed as: $M_3 = 3$ TeV, $\sqrt{F} = 20$ TeV, $K_p = 2$, (a) $\theta = 0.02$, (b) $\theta = 0.2$.

with

$$\sigma_0 = \frac{\pi}{32}\left|\frac{M_3}{F} + \frac{\alpha_s(m_s)\theta}{6\pi v} A\left(\frac{4m_t^2}{m_s^2}\right)\right|^2, \quad \tau = \frac{m_s^2}{S}. \tag{3.2}$$

Here $\sqrt{S}$ is the center-of-mass energy in pp collisions and $A\left(\frac{4m_t^2}{m_s^2}\right)$ is the loop factor (see, e.g. [41])

$$A(\tau_q) = \frac{3}{2}\tau_q\left(1 + (1-\tau_q)\, f(\tau_q)\right),$$

with

$$f(\tau_q) = \begin{cases} \arcsin^2 \frac{1}{\sqrt{\tau_q}}, & \text{if } \tau_q \geq 1 \\ -\frac{1}{4}\left[\log\frac{1+\sqrt{1-\tau_q}}{1-\sqrt{1-\tau_q}} - i\pi\right]^2, & \text{if } \tau_q < 1. \end{cases}$$

Note that with the mixing angle θ given by (2.31) both amplitudes in (3.2) are of the same order in $1/F$ and in the loop part of the amplitude we leave only the dominant contribution with the heavy top quark loop. As we assume the superpartners (in particular, squarks) to be relatively heavy, their contribution to this process is negligible.

The NLO corrections to the production cross section for a scalar which has both effective gluon interaction (2.37) and Yukawa interaction with top quark was calculated in [43] (see also refs. [44, 45] for the alternative calculation of the QCD corrections to this process). According to these results, corresponding K-factor, i.e. $K_p = \sigma_{NLO}/\sigma_{LO}$, is about 2 for chosen sgoldstino mass interval and $\sqrt{S} = 13, 14$ TeV. Since dependence of the K-factor on the relevant parameters in the considered parameter space is weak, we use the value $K_p = 2$ to correct the leading order sgoldstino production cross section calculated using CTEQ6 Parton Distribution Functions (the CTEQ6L1 PDF-set for computations in the leading order) [42].

The scalar sgoldstino production cross section is shown in figure 2 for the fixed values of parameters $M_3 = 3$ TeV, $\sqrt{F} = 20$ TeV, for center-of-mass energies $\sqrt{S} = 8$, 13, 14 and 28 TeV as well as for two values of the mixing angle $\theta = 0.02$ (left panel (a)) and 0.2 (right panel (b)). In the case of relatively small sgoldstino-Higgs mixing the cross section

JHEP05(2020)092

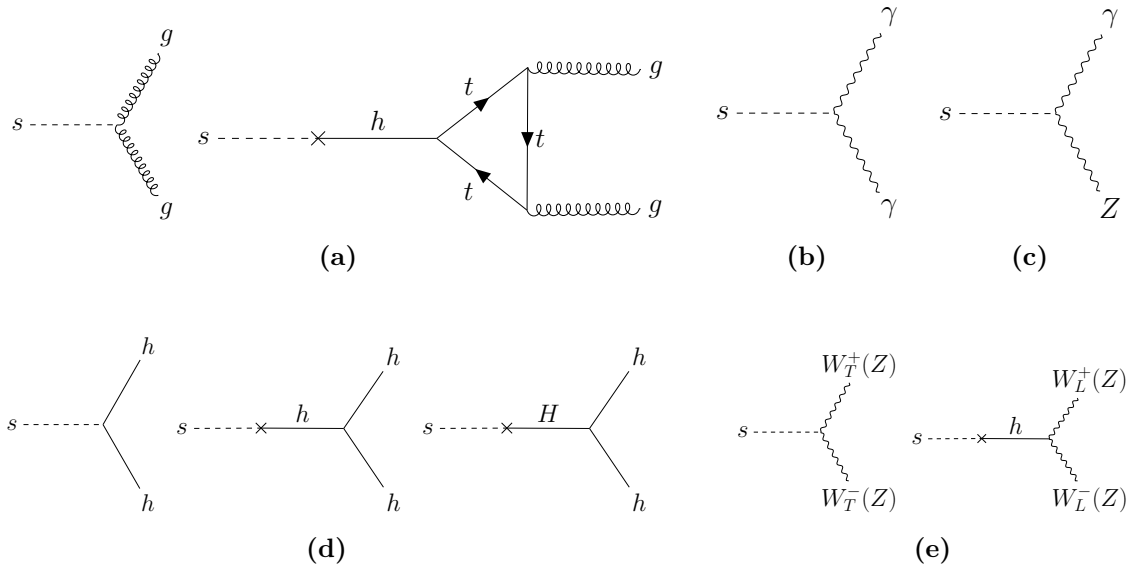

Figure 3. Feynman diagrams for main sgoldstino decay channels.

of sgoldstino production presented in figure 2a is dominated by the first term in (3.2), see figure 1a. In the opposite case of large mixing angle, the cross section in figure 2b reveals a non-trivial behavior related to the sgoldstino mass dependent contribution from the loop factor in the amplitude with sgoldstino-Higgs mixing, cf. figure 1b. For light sgoldstinos, the contribution from the mixing term dominates in the production cross section, see figure 1b. The effect is reduced with increasing sgoldstino mass and almost disappears as m_s approaches 1 TeV, where the first term in (3.2), figure 1a, fully dominates.

Other sgoldstino production channels [29] include vector boson fusion, sgoldstino associated production with a vector boson and $t\bar{t}s$ production. They are suppressed as compared to gluon fusion for the parameter space discussed in this study (even the sgoldstino-Higgs mixing does not change the day). In the considered region of sgoldstino mass m_s the gluon fusion gives the dominant contribution to production of virtual Higgs boson that mixes with sgoldstino. Since we consider regime of small values of mixing angle θ, the diagrams with sgoldstino-Higgs mixing are accordingly suppressed as compared to one in figure 1a. Therefore we consider for them only the gluon fusion channel of Higgs boson production.

3.2 Sgoldstino decays

Let us discuss the main decay modes of (sub)TeV sgoldstinos. The Feynman diagrams for the dominant decay channels are shown in figure 3. Corresponding amplitudes are determined by the interactions (2.36) and sgoldstino-Higgs mixing. The latter is taken into account in the analysis to the leading order in $1/F$.

We start with the sgoldstino decay into a pair of gluons, $s \to gg$. As in the case of sgoldstino production in gluon fusion there are two amplitudes in the leading order. Indeed, sgoldstino can decay directly into gluons or via mixing with the lightest Higgs

JHEP05(2020)092

boson, see figure 3a. Since in the leading order the decay to gluons is just the process cross symmetric to the gluon fusion, we find in the formula for sgoldstino rate to gluons the similar expression as in formula for production cross section (3.2), namely

$$\Gamma\left(s \to gg\right) = \frac{1}{4\pi}\left|\frac{M_3}{F} + \frac{\alpha_s(m_s)\theta}{6\pi v} A\left(\frac{4m_t^2}{m_s^2}\right)\right|^2 m_s^3. \tag{3.3}$$

In the absence of the mixing (i.e. when $\theta = 0$) this expression can be found in ref. [36]. We include NLO QCD corrections by introducing the factor $K_d = 1.6$ for gluon decay channel of sgoldstino. In the considered regime of sgoldstino decaying dominantly into Higgs and massive vector bosons, its precise value is not very important and we conservatively choose it close to that of predicted for gluonic decay of the Higgs-like scalar (see figure 7 in [41]).

In the sgoldstino decays to either pair of photons $s \to \gamma\gamma$ (figure 3b), or photon and Z-boson $s \to \gamma Z$ (figure 3c), we can neglect the mixing contribution, since the Higgs boson h decays into these particles through loops and the corresponding amplitudes are highly suppressed by gauge and loop factors. Therefore, the corresponding decay widths reads [36]

$$\Gamma\left(s \to \gamma\gamma\right) = \frac{1}{32\pi}\frac{1}{F^2} M_{\gamma\gamma}^2 m_s^3, \tag{3.4}$$

$$\Gamma\left(s \to \gamma Z\right) = \frac{1}{16\pi}\frac{M_{Z\gamma}^2}{F^2} m_s^3 \left(1 - \frac{m_Z^2}{m_s^2}\right)^3. \tag{3.5}$$

Next we consider the scalar sgoldstino to be heavy enough for the decay into a pair of the lightest Higgs bosons (figure 3d). The decay width can be calculated with help of the trilinear coupling in eq. (2.35) as

$$\Gamma(s \to hh) = \frac{C_{\tilde{s}\tilde{h}\tilde{h}}^2}{8\pi m_s}\sqrt{1 - \frac{4m_h^2}{m_s^2}}\,. \tag{3.6}$$

The case of sgoldstino decays to massive vector bosons is more involved [36]. Let us consider the decay of sgoldstino into a pair of W-bosons (figure 3e). The sgoldstino Lagrangian contains two different terms responsible for the interaction between sgoldstino and W-bosons. The first one is the contribution of the first term in (2.36) which is determined by the coupling constant

$$C_{sWW_T} = -\frac{M_2}{F\sqrt{2}}. \tag{3.7}$$

This term originates from the sgoldstino interaction Lagrangian (2.36) and is not affected by mixing with the neutral Higgs bosons (to the leading order in $1/F$). Another contribution is related to sgoldstino-Higgs mixing and the interactions of the Higgs bosons with $W^{\pm}$. The corresponding interaction Lagrangian has the form

$$C_{sWW_L} m_W^2 W^\mu W_\mu\, s \equiv \left(-\theta\frac{\sqrt{2}}{v}\sin(\beta-\alpha) - \psi\frac{\sqrt{2}}{v}\cos(\beta-\alpha)\right) m_W^2 W^\mu W_\mu\, s. \tag{3.8}$$

JHEP05(2020)092

The width of $s \to W^+W^-$ decay from both contributions is given by the formula

$$\Gamma(s \to WW) = \frac{1}{16\pi}\frac{m_W^4}{m_s}\left[2C_{sWW_T}^2\left(6-4\frac{m_s^2}{m_W^2}+\frac{m_s^4}{m_W^4}\right)-\right.$$
$$\left.-12C_{sWW_T}C_{sWW_L}\left(1-\frac{m_s^2}{2m_W^2}\right)+C_{sWW_L}^2\left(3-\frac{m_s^2}{m_W^2}+\frac{m_s^4}{4m_W^4}\right)\right]\sqrt{1-\frac{4m_W^2}{m_s^2}}\,. \tag{3.9}$$

Similarly for Z-boson one obtains

$$\Gamma(s \to ZZ) = \frac{1}{8\pi}\frac{m_Z^4}{m_s}\left[2C_{sZZ_T}^2\left(6-4\frac{m_s^2}{m_Z^2}+\frac{m_s^4}{m_Z^4}\right)-\right.$$
$$\left.-12C_{sZZ_T}C_{sZZ_L}\left(1-\frac{m_s^2}{2m_Z^2}\right)+C_{sZZ_L}^2\left(3-\frac{m_s^2}{m_Z^2}+\frac{m_s^4}{4m_Z^4}\right)\right]\sqrt{1-\frac{4m_Z^2}{m_s^2}}. \tag{3.10}$$

The respective trilinear coefficients for Z-bosons are

$$C_{sZZ_T} = -\frac{M_1\sin^2\theta_W + M_2\cos^2\theta_W}{2\sqrt{2}F}, \tag{3.11}$$

$$C_{sZZ_L} = -\frac{\theta}{v\sqrt{2}}\sin(\beta-\alpha) - \frac{\psi}{v\sqrt{2}}\cos(\beta-\alpha). \tag{3.12}$$

The decay widths of sgoldstino to fermions $s \to f\bar{f}$ are small as compared to the decay widths to bosons. Also note that sgoldstino can decay into pair of gravitinos, however the corresponding partial width is strongly suppressed in the interesting case of $m_s \ll \sqrt{F}$. In summary, the total sgoldstino decay width can be found as the following sum over all the considered decay channels

$$\Gamma_{\rm tot} = \Gamma(s \to gg) + \Gamma(s \to \gamma\gamma) + \Gamma(s \to \gamma Z) + \Gamma(s \to hh) + \Gamma(s \to WW) + \Gamma(s \to ZZ)\,. \tag{3.13}$$

The total width scales as $1/F^2$ and for $m_{soft}, \mu \ll \sqrt{F}$ sgoldstino width is typically considerably smaller than its mass.

Let us discuss how the hierarchy between different sgoldstino decay modes depends on its mixing with other part of the Higgs sector. It is known that at large $\sqrt{F}$ even small mixing with the Higgs bosons can change the patterns of dominant sgoldstino decay modes [38]. In our analysis we concentrate mostly on the decoupling regime, i.e. when $m_A, m_H \gg m_h$, which corresponds to $\sin\alpha \approx -\cos\beta$ and $\cos\alpha \approx \sin\beta$. In this limit, along with $m_{soft}, \mu \ll \sqrt{F}$ which is required for small values of the mixing angles, the scalar sgoldstino of the mass at TeV scale mixes mainly with the lightest Higgs boson. The corresponding mixing angle determines the parameter X in (2.19) which becomes

$$X = -v\left(\frac{g_1^2M_1 + g_2^2M_2}{2}v^2\cos^2 2\beta + 2\mu^3\sin 2\beta\right). \tag{3.14}$$

For the part of the model parameter space relevant for our study the last term in this expression dominates. To illustrate the hierarchy between the sgoldstino decay modes, we

JHEP05(2020)092

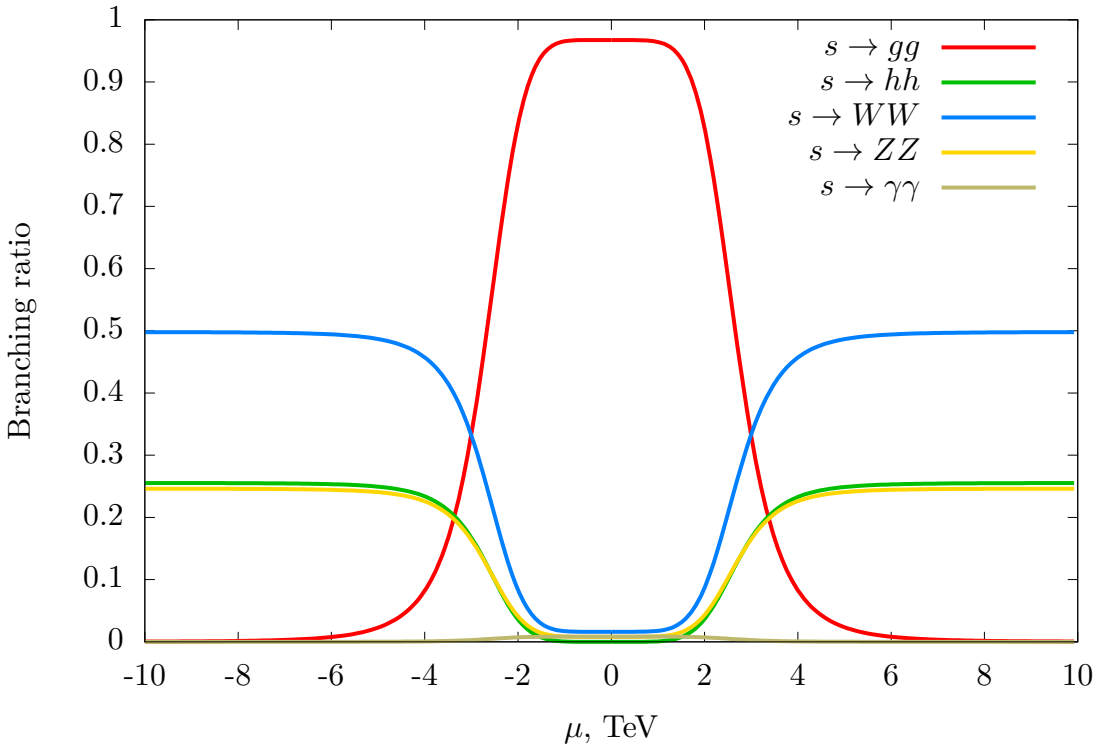

Figure 4. Branching ratios for sgoldstino decays in two gluons ($s \to gg$, red line), two light neutral Higgs bosons ($s \to hh$, green line), two W-bosons ($s \to WW$, blue line), two Z-bosons ($s \to ZZ$, yellow line), two photons ($s \to \gamma\gamma$, brown line) versus parameter μ. Here the model parameters are fixed as follows: $\tan\beta = 10$, $m_s = 1\,\text{TeV}$, $m_A = 5\,\text{TeV}$, $M_1 = M_2 = 1\,\text{TeV}$, $M_3 = 3\,\text{TeV}$, $\sqrt{F} = 20\,\text{TeV}$, K-factor for gg channel equals $K_d = 1.6$.

show in figure 4 their branching ratios as functions of the parameter μ. Here the values of other model parameters are fixed as $\tan\beta = 10$, $m_A = 5\,\text{TeV}$, $M_1 = M_2 = 1\,\text{TeV}$, $M_3 = 3\,\text{TeV}$, $\sqrt{F} = 20\,\text{TeV}$, $K_d = 1.6$ and sgoldstino mass is $m_s = 1\,\text{TeV}$. We observe two different regimes of possible sgoldstino decays. At relatively small values of μ and therefore small sgoldstino-Higgs mixing, sgoldstino decays dominantly into gluons, whereas the partial widths of the other decay channels and, in particular, the decay into two light neutral Higgs bosons, are suppressed. Note, that most of the previous studies of sgoldstino phenomenology in high energy collisions assumed gluon dominance in sgoldstino decays. In the opposite case of large absolute values of μ, i.e. with a considerable admixture of the Higgs bosons in sgoldstino, the latter decays mainly into heavy particles of the electroweak sector, namely, the Higgs hh and massive vector W^+W^-, ZZ bosons. In the decoupling limit the corresponding partial decay widths are related approximately as 1:2:1 respectively. This regime was discussed in ref. [35] in the context of searches for sgoldstino at the LHC. Our present interest in this study is related to the possibility of resonant double Higgs production in this part of the model parameter space, as the branching ratio of two light neutral Higgs boson channel can reach 25%. Note that in this regime sgoldstino decays also into massive vector bosons which can help to test this scenario.

JHEP05(2020)092

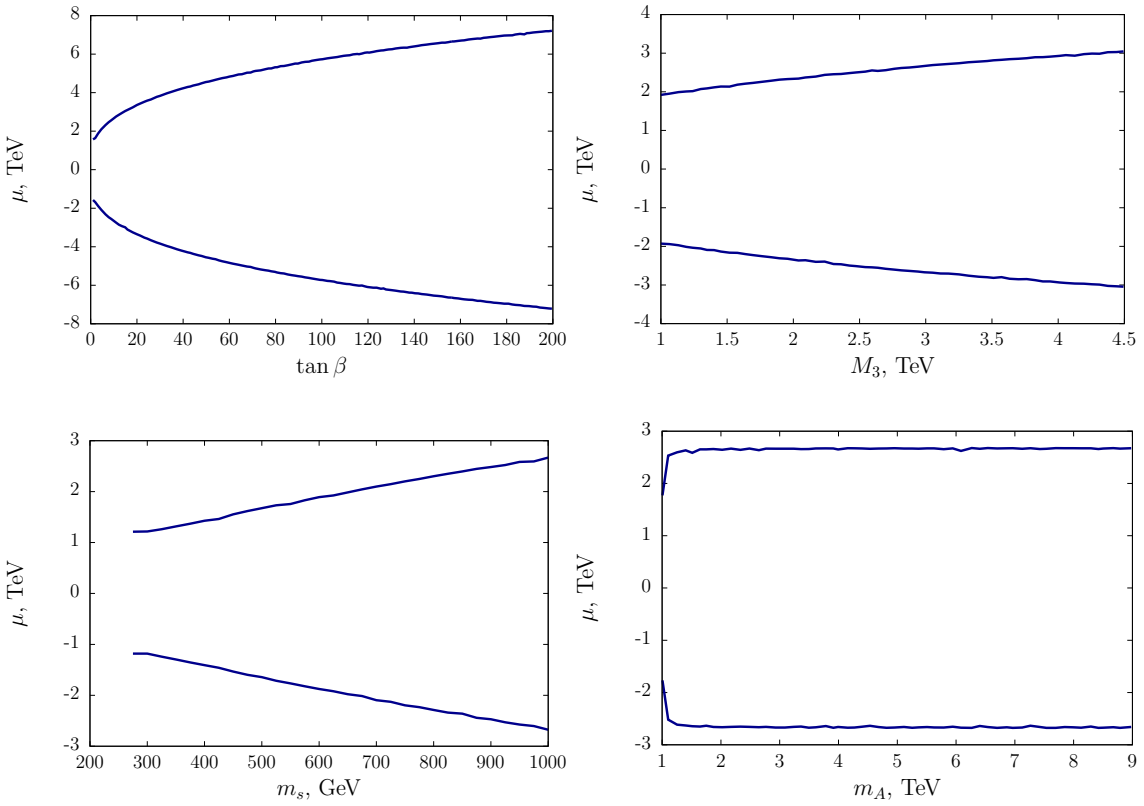

Figure 5. Slices of the conditional boundary $Br(s \to hh) = 0.125$ between gluon dominated and massive boson dominated regimes of sgoldstino decay on the planes $(\tan\beta, \mu)$ (upper left panel), (M_3, μ) (upper right panel), (m_s, μ) (lower left panel) and (m_A, μ) (lower right panel). Regions between the lines on the plots correspond to the gluon dominated sgoldstino decay. Other model parameters are fixed as $\tan\beta = 10$, $m_A = 5\,\text{TeV}$, $m_s = 1\,\text{TeV}$, $M_3 = 3\,\text{TeV}$, $M_1 = M_2 = 1\,\text{TeV}$, $\sqrt{F} = 20\,\text{TeV}$. K-factor for gg channel is $K_d = 1.6$.

In this calculation we use the approximate formulas for mixing angles for simplicity. We checked this approximation by computing mixing angles using (exact) numerical diagonalization of the mass matrix. The results from approximate formulas agree very well with branching ratios obtained numerically.

Let us study the dependence of the transition between gluon dominated and heavy boson dominated regimes of sgoldstino decays on the model parameters. As a conditional boundary between these two regimes we take $Br(s \to hh) = 0.125$ and in figure 5 we show slices of this boundary on the planes $(\tan\beta, \mu)$, (M_3, μ), (m_s, μ) and (m_A, μ) assuming other parameters to be fixed. Regions between the lines on the plots correspond to smaller $|\mu|$ and therefore to the gluon dominated sgoldstino decay. Outside these regions sgoldstino decays mostly to hh, W^+W^- and ZZ and the ratio between their partial widths approaches 1:2:1 at larger $|\mu|$. We see that larger values of $\tan\beta, M_3, m_s$ push the boundary of the region with gluon dominated sgoldstino decay to larger values of μ. A nontrivial dependence of the boundaries on m_A is observed only for its small values, when the decoupling regime gets violated.

JHEP05(2020)092

Let us present analytical estimates for the dependence of the boundaries between different regimes on the model parameters. At large mixing angle the leading contribution to the sgoldstino decay width into two W-bosons (3.9) for $m_s \gg m_W$ is

$$\Gamma(s \to WW) \sim \frac{1}{4\pi}\frac{\theta^2}{8v^2} m_s^3 \,. \tag{3.15}$$

The vector bosons dominate in sgoldstino decays if $\Gamma(s \to gg) \ll \Gamma(s \to WW)$ or

$$\left| \frac{2M_3 v}{F\theta} + \frac{\alpha_s A_t}{3\pi} \right| \ll 1 \,, \tag{3.16}$$

where we denote $A\left(4m_t^2/m_s^2\right) = A_t$ for brevity. For all values of sgoldstino mass in the range 200–1000 GeV we find $|A_t| \leq 1.9$ and $\alpha_s A_t/(3\pi) \ll 1$. Therefore, the condition of dominating decays of sgoldstino to vector bosons is $|\theta| \gg \theta_{\rm cr}$, where

$$\theta_{\rm cr} = 2\sqrt{2}\frac{M_3 v}{F}. \tag{3.17}$$

4 Phenomenology of the resonant sgoldstino signature

In this section we discuss sgoldstino production at the LHC yielding the resonant signatures in hh, W^+W^- and ZZ final states. Our primary interest here is in double-Higgs mode, which we start from; the other two we investigate similarly. Also recall, that sgoldstino partial decay widths for these double-boson final states are related as 1:2:1 for $\theta \gg \theta_{\rm cr}$, and so the modes are compatible. To calculate the cross section of the resonant di-Higgs production in the process $pp \to s \to hh$, we work in the narrow width approximation for sgoldstino which means that the cross section for production of particles in a final state fin is found as a product of the sgoldstino production cross section (at the given energy of protons) and the corresponding branching ratio $\mathrm{Br}(s \to fin)$.

The dependence of the resonant double Higgs boson production cross section on μ for chosen values of $\tan\beta$ and M_3 is shown in figures 6a and 6b. Other parameters are fixed as follows: $m_s = 1\,\mathrm{TeV}$, $m_A = 5\,\mathrm{TeV}$, $M_1 = M_2 = 1\,\mathrm{TeV}$, $\sqrt{F} = 20\,\mathrm{TeV}$, $K_p = 2$, $K_d = 1.6$. We see that for small values of $|\mu|$ the cross section of this process is relatively small due to a suppression of the decay channel $s \to hh$. At the same time, the cross section is increased for larger $|\mu|$, i.e. for larger mixing between sgoldstino and the lightest Higgs boson (3.14) which corresponds to transition to the regime of sgoldstino decay to massive vector bosons. It is in this regime the resonant cross sections of $pp \to s \to W^+W^-$ and $pp \to s \to ZZ$ are directly related to that of di-Higgs production. As it can be seen from figure 6a, with the increase of $\tan\beta$, the value of μ, at which the double Higgs production is enhanced, also increases. The sgoldstino production cross section grows with M_3 and therefore the double Higgs production cross section also increases.

At large values of M_3 the points with large absolute values of μ in figure 6b are excluded by existing experimental data obtained by ATLAS and CMS collaborations. The search for a scalar resonance that decays to two W-bosons was performed in [46, 47]. Scalar resonance decaying into ZZ was studied in [48]; see also refs. [49] for [50] the case of Z-boson

JHEP05(2020)092

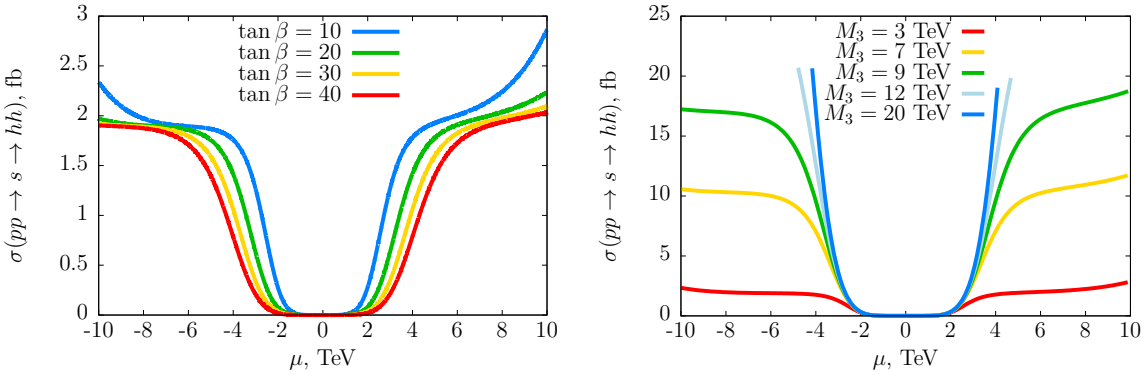

(a) **(b)**

Figure 6. Resonant di-Higgs production cross section of the process $pp \to s \to hh$ as a function of μ for different values of $\tan\beta$ (a) and M_3 (b), calculated for $\sqrt{S} = 13\,\text{TeV}$. Other parameters are fixed as $m_s = 1\,\text{TeV}$, $m_A = 5\,\text{TeV}$, $M_1 = M_2 = 1$ TeV, $\sqrt{F} = 20\,\text{TeV}$, $K_p = 2$, $K_d = 1.6$; $M_3 = 3\,\text{TeV}$ (a) and $\tan\beta = 10$ (b).

and photon in the final state and ref. [51] for a pair of photons. We also take into account current upper limits on the production cross section of a scalar which decays into two Higgs bosons which are presented in [52–58]. We use the whole set of the above experimental constraints to find the phenomenologically viable region in the model parameter space. In figures 6a, 6b we show the results for phenomenologically viable models only.

One can notice that the cross section in figure 6a is nearly constant at intermediate absolute values of μ but starts growing again at its larger absolute values. This behavior is due to the change in the dominant contribution to the sgoldstino effective coupling to gluons. Namely, according to (2.19) and (2.31) the larger values of $|\mu|$ correspond to larger $|X|$ and $|\theta|$. In this regime, the cross section of sgoldstino production (3.1) is determined mostly by the sgoldstino mixing with the Higgs boson. Parametrically this occurs when

$$\frac{M_3}{F} \ll \frac{\alpha_s|\theta||A_t|}{6\pi v}, \tag{4.1}$$

or $|\theta| \gg \theta'_{\text{cr}}$ with $\theta'_{\text{cr}} \equiv 6\pi v M_3/(\alpha_s|A_t|F)$. Thus for θ larger than the critical value θ'_{cr}, the sgoldstino production cross section increases with the growth of $|\mu|$. For $\theta_{\text{cr}} \ll \theta'_{\text{cr}}$, this cross section does not depend on the value of the mixing angle and it is determined fully by values of sgoldstino mass, M_3 and F.

In figure 7 we show the similar dependencies of the cross section $pp \to s \to hh$ as in figure 6 but calculated for $\sqrt{S} = 14\,\text{TeV}$. The cross section is depicted for five different combinations of $\tan\beta$ and M_3 and for the same set of other parameters. Similarly, in figure 8 the cross sections of the processes $pp \to s \to WW$ and $pp \to s \to ZZ$ are calculated for $\sqrt{S} = 14\,\text{TeV}$. Let us note again that at $\theta > \theta_{\text{cr}}$ the following relations between the resonant sgoldstino production cross sections

$$\sigma(pp \to s \to W^+W^-) \approx 2\sigma(pp \to s \to ZZ) \approx 2\sigma(pp \to s \to hh) \tag{4.2}$$

are valid.

JHEP05(2020)092

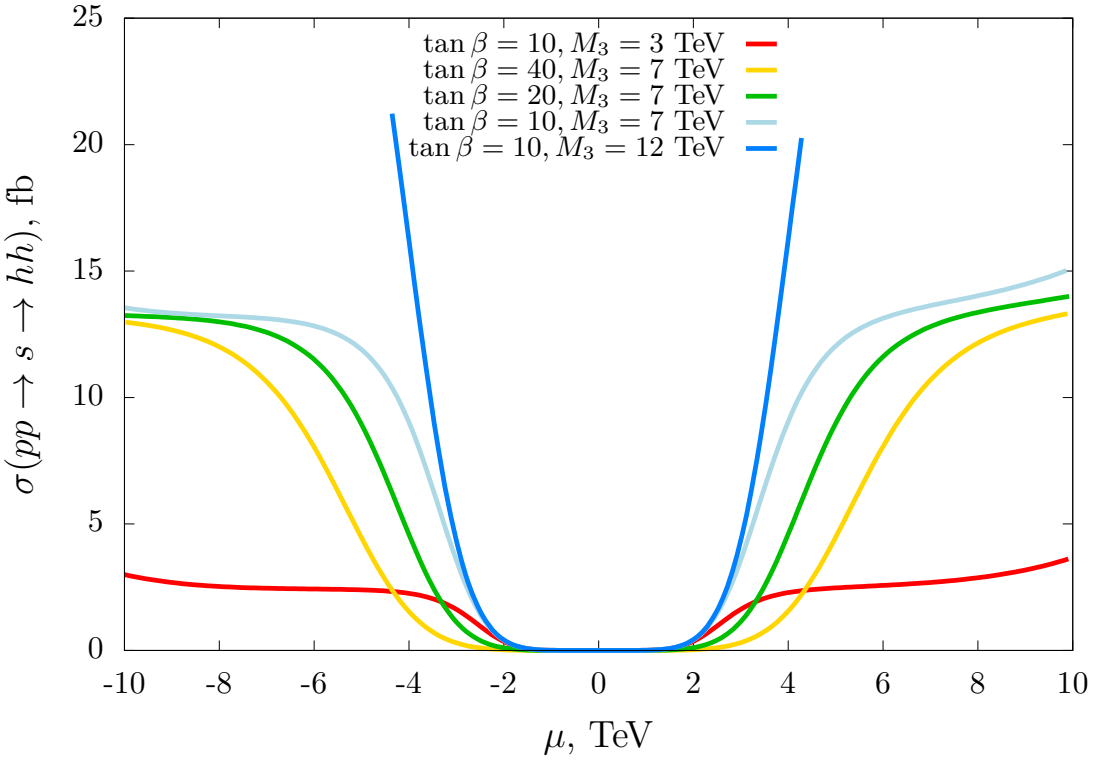

Figure 7. Resonant di-Higgs production cross section of the process $pp \to s \to hh$ calculated for $\sqrt{S} = 14\,\text{TeV}$. The model parameters are chosen as $m_s = 1\,\text{TeV}$, $m_A = 5\,\text{TeV}$, $M_1 = M_2 = 1\,\text{TeV}$, $\sqrt{F} = 20$ TeV, $K_p = 2$, $K_d = 1.6$.

In the rest of this section we assume the regime of sgoldstino decaying dominantly into hh, W^+W^- and ZZ with the relation 1:2:1 between their partial widths. In this regime, the results of searches for neutral scalar resonances by the ATLAS and the CMS collaborations at $\sqrt{S} = 13\,\text{TeV}$ discussed above can be used to constrain sgoldstino production cross section and corresponding parameters of the model. Assuming $\theta \gg \theta_{\text{cr}}$ (which corresponds to the regime 1:2:1 for sgoldstino decays) as well as $\theta \ll \theta'_{\text{cr}}$ (meaning that the first term in the expression (3.2) for the sgoldstino production cross section dominates) one obtains that the cross section depends on the combination M_3/F only. Hence the experimental data can be used to constrain this quantity.

$$\left[\frac{M_3/3\text{ TeV}}{(\sqrt{F}/20\text{ TeV})^2}\right]^{\max} = \sqrt{\frac{\sigma^{\max}_{\text{prod}}}{\sigma'_{\text{prod}}}} \leq \sqrt{\frac{\sigma^{\max}_{XX}}{\sigma'_{\text{prod}} Br(s \to XX)}}, \tag{4.3}$$

here σ'_{prod} is the sgoldstino production cross section for $M_3 = 3\,\text{TeV}$, $\sqrt{F} = 20\,\text{TeV}$, and X runs through $\{h, W, Z\}$. The obtained constraints are presented in figure 9. In the case of not very heavy sgoldstinos ($m_s \lesssim 600\,\text{GeV}$) the most rigorous constraints are given by the decay mode $s \to hh$.

Using lower limits on M_3 from the searches for gluino in models with gauge-mediated supersymmetry breaking along with the upper bound on M_3/F presented above one can obtain constraints on the supersymmetry breaking scale $\sqrt{F}$. In most of the experimental

JHEP05(2020)092

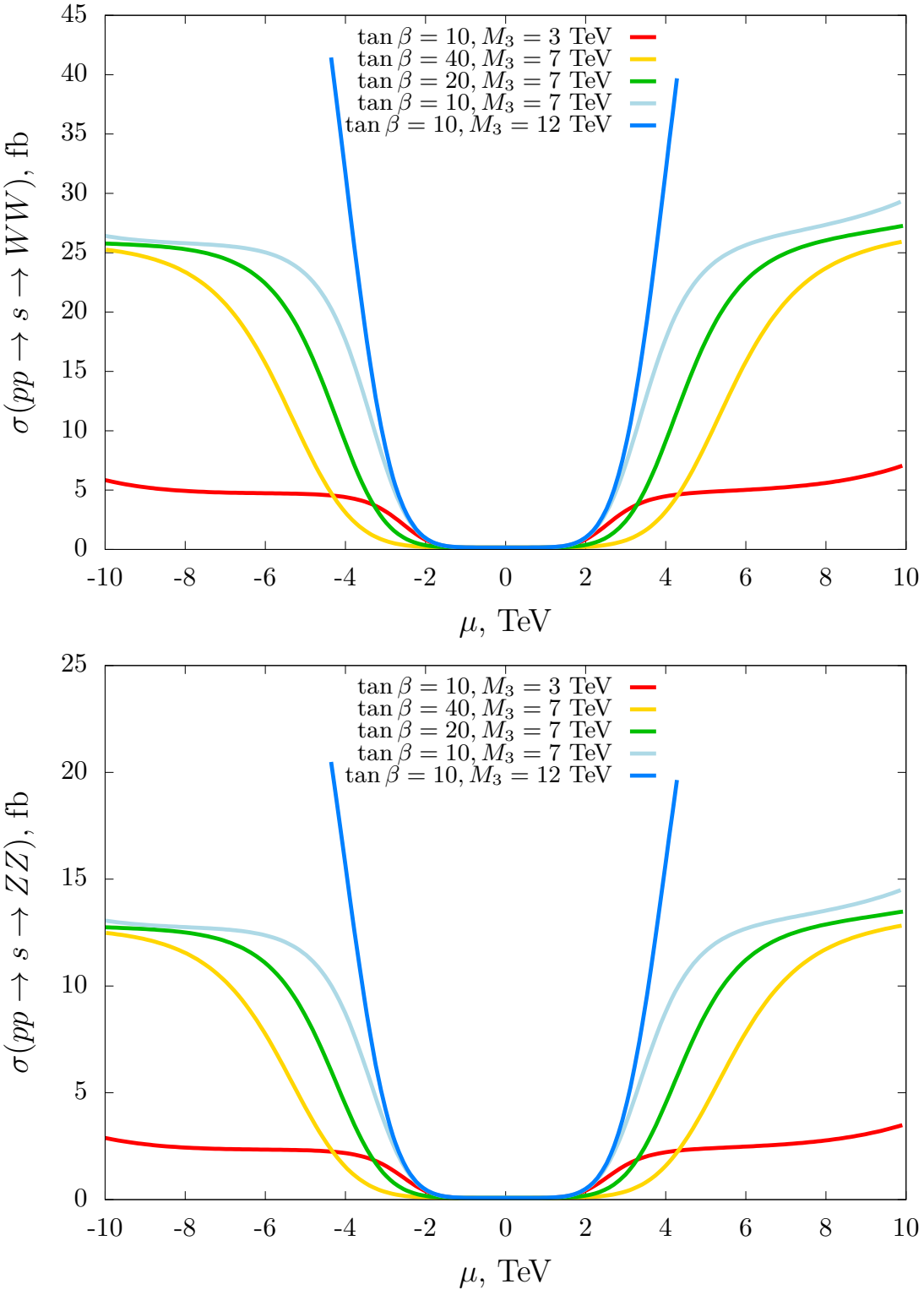

Figure 8. Resonant production cross section of the processes $pp \to s \to WW$ (upper panel), $pp \to s \to ZZ$ (lower panel) calculated for $\sqrt{S} = 14\,\text{TeV}$. The model parameters are chosen as $m_s = 1\,\text{TeV}$, $m_A = 5\,\text{TeV}$, $M_1 = M_2 = 1\,\text{TeV}$, $\sqrt{F} = 20\,\text{TeV}$, $K_p = 2$, $K_d = 1.6$.

JHEP05(2020)092

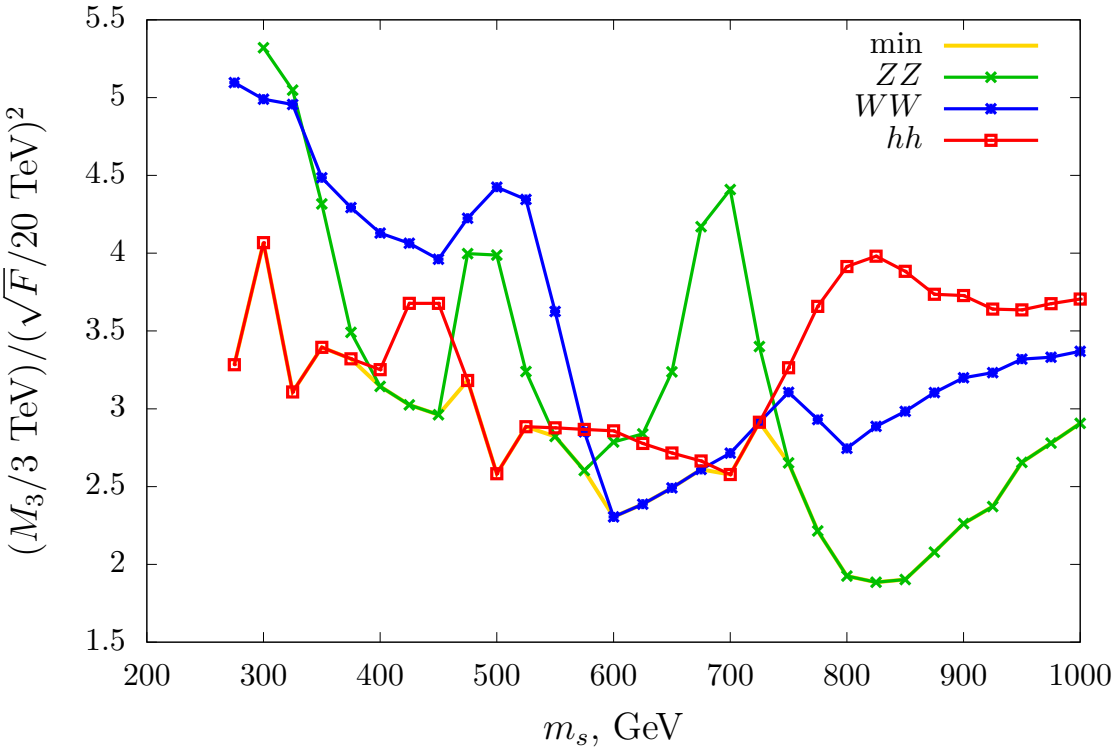

Figure 9. Upper limits at 95% CL on ratio M_3/F obtained from the experimental data [46–48, 52–58] for $\sqrt{S} = 13\,\mathrm{TeV}$. Constraints obtained from the searches for a heavy scalar resonance decaying into a pair of Z-bosons, W-bosons and Higgs bosons are shown in green, blue and red, respectively. The yellow line connects points of joint constraint on M_3/F (minimum upper limit).

studies [59–65] lower limits on gluino mass were obtained for several simplified models and the presented experimental bound varies in the range 1.8–2 TeV. Adopting for the estimate the conservative lower bound $(M_3)_{LL} > 2\,\mathrm{TeV}$ and using the constraints on M_3/F from $\sqrt{S} = 13\,\mathrm{TeV}$ data shown in figure 9, we apply

$$F(m_s) \geq \frac{(M_3)_{LL}}{(M_3/F)_{UL}(m_s)}, \tag{4.4}$$

to find lower bounds on $\sqrt{F}$ depending on the mass of the scalar sgoldstino, which are shown in figure 10. We find that in the considered part of the model parameter space the bounds on $\sqrt{F}$ varies in 8–12 TeV range.

5 Conclusions

To summarize, in this work we have investigated the impact of sgoldstino-Higgs mixing on sgoldstino decays and production in proton-proton collisions. We have observed two different regimes in sgoldstino decays. At the small mixing sgoldstino decays dominantly into gluons while at the large one it decays into the lightest Higgs bosons and vector bosons, W^+W^- and ZZ, with the relation between the corresponding branching ratios as 1:2:1. In

JHEP05(2020)092

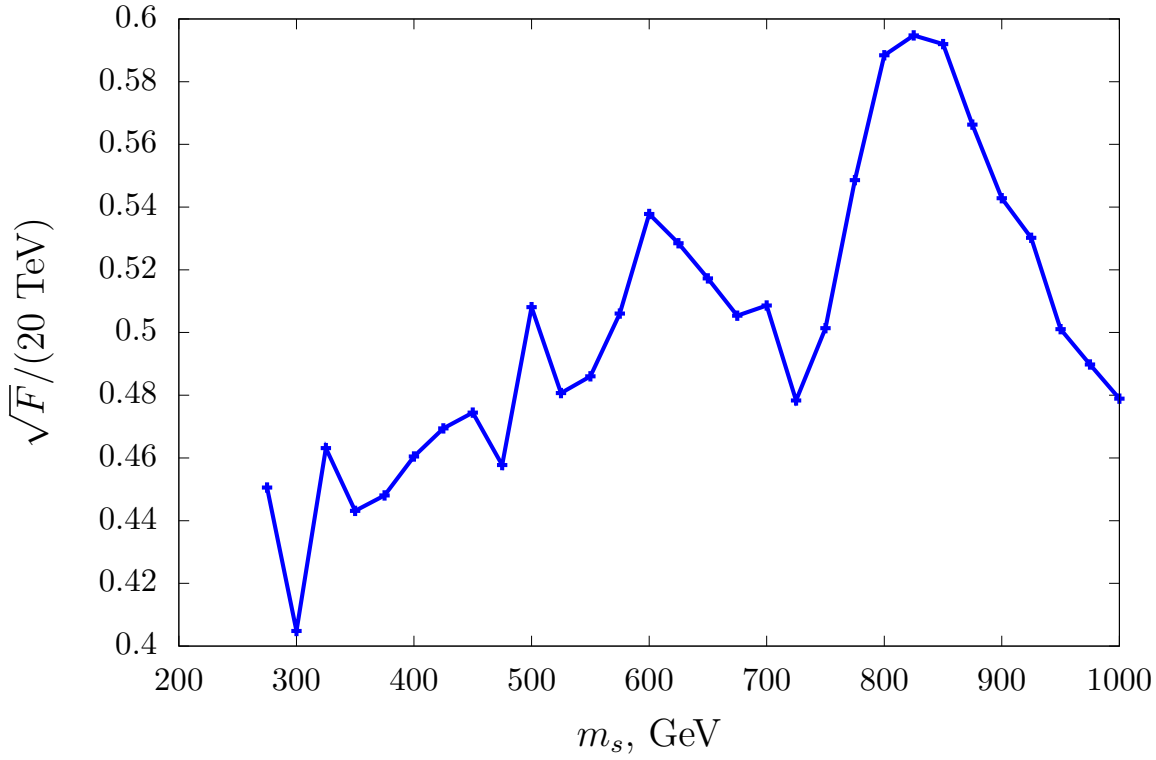

Figure 10. Lower limit on $\sqrt{F}$ obtained using the upper limit on M_3/F (figure 9) and a conservative lower bound $M_3 \gtrsim 2\,\mathrm{TeV}$ from experimental data [59–65] at $\sqrt{S} = 13\,\mathrm{TeV}$.

this region of the model parameter space there can be enhanced resonant di-Higgs production. Using current experimental data from the LHC experiments we obtained constraint on the ratio M_3/F. With the current conservative constraint $M_3 \gtrsim 2\,\mathrm{TeV}$ we placed the bounds on the supersymmetry breaking scale $\sqrt{F}$ varying in 8–12 TeV range for sgoldstino of masses 200–1000 GeV and in the regime of massive boson dominance in its decays. Since $\sqrt{F}$ can be treated as a scale of SUSY breaking, the estimate of its lower limit may be useful for a theoretical consideration of similar low-scale supersymmetry breaking models with sgoldstino. A characteristic signature of the considered scenario is the appearance of sgoldstino resonance in di-Higgs, W^+W^- and ZZ spectra with the relation between corresponding cross section close to 1:2:1. Searches for the resonant production of massive boson resonances at HL-LHC are expected to either reveal the sgoldstino signature or put further constraints on the models with sgoldstino using updated results of experimental searches for this process.

Acknowledgments

The work of EK was supported by the grant of "BASIS" Foundation no. 19-2-6-16-1.

JHEP05(2020)092

A Trilinear coefficients for a set of sgoldstino-Higgs bosons vertices

$$shH\times C_{shH}\equiv\frac{shH}{F\sqrt{2}}\left(\frac{v^2}{2}\left(g_1^2M_1+g_2^2M_2\right)\left(2\sin2\alpha\cos2\beta+\cos2\alpha\sin2\beta\right)+\right.$$
$$\left.+\mu(m_A^2-2\mu^2)\cos2\alpha\right), \tag{A.1}$$

$$sAA\times C_{sAA}\equiv\frac{sAA}{F\sqrt{2}}\left(\frac{v^2}{4}(g_1^2M_1+g_2^2M_2)\cos^2 2\beta-\mu\sin2\beta(m_A^2-\mu^2)\right), \tag{A.2}$$

$$sH^+H^-\times C_{sH^+H^-}\equiv\frac{sH^+H^-}{F\sqrt{2}}\left(-g_2^2M_2v^2(1+\sin2\beta)-2\mu\left(m_A^2(1+\sin2\beta)-2\mu^2\right)\right), \tag{A.3}$$

$$pAH\times C_{pAH}\equiv\frac{pAH}{F\sqrt{2}}\mu(m_A^2-2\mu^2)\cos(\alpha-\beta), \tag{A.4}$$

$$pAh\times C_{pAh}\equiv\frac{pAh}{F\sqrt{2}}\mu(m_A^2-2\mu^2)\sin(\beta-\alpha). \tag{A.5}$$

B Trilinear coefficients in the mass basis for a set of sgoldstino-Higgs bosons vertices

$$\frac{\tilde{s}\tilde{h}\tilde{H}}{F}\left(C_{shH}-2C_{hhH}\theta-2C_{hHH}\psi\right), \tag{B.1}$$

$$\frac{\tilde{s}\tilde{A}\tilde{A}}{F}\left(C_{sAA}-C_{hAA}\theta-C_{HAA}\psi\right), \tag{B.2}$$

$$\frac{\tilde{s}\tilde{H}^+\tilde{H}^-}{F}\left(C_{sH^+H^-}-C_{hH^+H^-}\theta-C_{HH^+H^-}\psi\right), \tag{B.3}$$

$$\frac{\tilde{p}\tilde{A}\tilde{H}}{F}\left(C_{pAH}-2C_{HAA}\xi\right), \tag{B.4}$$

$$\frac{\tilde{p}\tilde{A}\tilde{h}}{F}\left(C_{pAh}-2C_{hAA}\xi\right), \tag{B.5}$$

where definitions of trilinear coefficients for vertices with one sgoldstino and two Higgs bosons can be found in appendix A, C_{hhH} and C_{hHH} are introduced in (2.25), (2.26), the remaining MSSM trilinear coefficients are listed below,

$$C_{hH^+H^-}\equiv\frac{1}{\sqrt{2}}g_2^2v\left(\cos\alpha-\sin\alpha\right)\left(\cos\beta+\sin\beta\right), \tag{B.6}$$

$$C_{HH^+H^-}\equiv\frac{1}{\sqrt{2}}g_2^2v\left(\cos\alpha+\sin\alpha\right)\left(\cos\beta+\sin\beta\right), \tag{B.7}$$

$$C_{hAA}\equiv\frac{1}{2\sqrt{2}}\frac{m_Z^2}{v}\cos2\beta\sin(\alpha+\beta), \tag{B.8}$$

$$C_{HAA}\equiv-\frac{1}{2\sqrt{2}}\frac{m_Z^2}{v}\cos2\beta\cos(\alpha+\beta). \tag{B.9}$$

JHEP05(2020)092

References

[1] ATLAS collaboration, *Observation of a new particle in the search for the Standard Model Higgs boson with the ATLAS detector at the LHC*, *Phys. Lett.* **B 716** (2012) 1 [arXiv:1207.7214] [INSPIRE].

[2] CMS collaboration, *Observation of a New Boson at a Mass of 125 GeV with the CMS Experiment at the LHC*, *Phys. Lett.* **B 716** (2012) 30 [arXiv:1207.7235] [INSPIRE].

[3] J. Alison et al., *Higgs Boson Pair Production at Colliders: Status and Perspectives*, in *Double Higgs Production at Colliders*, Batavia, IL, U.S.A., 4–9 September 2018, B. Di Micco, M. Gouzevitch, J. Mazzitelli and C. Vernieri eds. (2019) [arXiv:1910.00012] [INSPIRE].

[4] E.W.N. Glover and J.J. van der Bij, *Higgs boson pair production via gluon fusion*, *Nucl. Phys.* **B 309** (1988) 282 [INSPIRE].

[5] S. Dawson, S. Dittmaier and M. Spira, *Neutral Higgs boson pair production at hadron colliders: QCD corrections*, *Phys. Rev.* **D 58** (1998) 115012 [hep-ph/9805244] [INSPIRE].

[6] S. Borowka et al., *Higgs Boson Pair Production in Gluon Fusion at Next-to-Leading Order with Full Top-Quark Mass Dependence*, *Phys. Rev. Lett.* **117** (2016) 012001 [*Erratum ibid.* **117** (2016) 079901] [arXiv:1604.06447] [INSPIRE].

[7] D. de Florian and J. Mazzitelli, *Higgs Boson Pair Production at Next-to-Next-to-Leading Order in QCD*, *Phys. Rev. Lett.* **111** (2013) 201801 [arXiv:1309.6594] [INSPIRE].

[8] M. Grazzini et al., *Higgs boson pair production at NNLO with top quark mass effects*, *JHEP* **05** (2018) 059 [arXiv:1803.02463] [INSPIRE].

[9] L.-B. Chen, H.T. Li, H.-S. Shao and J. Wang, *Higgs boson pair production via gluon fusion at N^3LO in QCD*, *Phys. Lett.* **B 803** (2020) 135292 [arXiv:1909.06808] [INSPIRE].

[10] J.M. No and M. Ramsey-Musolf, *Probing the Higgs Portal at the LHC Through Resonant di-Higgs Production*, *Phys. Rev.* **D 89** (2014) 095031 [arXiv:1310.6035] [INSPIRE].

[11] C.-Y. Chen, S. Dawson and I.M. Lewis, *Exploring resonant di-Higgs boson production in the Higgs singlet model*, *Phys. Rev.* **D 91** (2015) 035015 [arXiv:1410.5488] [INSPIRE].

[12] K. Nakamura, K. Nishiwaki, K.-y. Oda, S.C. Park and Y. Yamamoto, *Di-Higgs enhancement by neutral scalar as probe of new colored sector*, *Eur. Phys. J.* **C 77** (2017) 273 [arXiv:1701.06137] [INSPIRE].

[13] I.M. Lewis and M. Sullivan, *Benchmarks for Double Higgs Production in the Singlet Extended Standard Model at the LHC*, *Phys. Rev.* **D 96** (2017) 035037 [arXiv:1701.08774] [INSPIRE].

[14] R. Grober, M. Muhlleitner and M. Spira, *Higgs Pair Production at NLO QCD for CP-violating Higgs Sectors*, *Nucl. Phys.* **B 925** (2017) 1 [arXiv:1705.05314] [INSPIRE].

[15] S. Dawson and M. Sullivan, *Enhanced di-Higgs boson production in the complex Higgs singlet model*, *Phys. Rev.* **D 97** (2018) 015022 [arXiv:1711.06683] [INSPIRE].

[16] P. Basler, S. Dawson, C. Englert and M. Mühlleitner, *Showcasing HH production: Benchmarks for the LHC and HL-LHC*, *Phys. Rev.* **D 99** (2019) 055048 [arXiv:1812.03542] [INSPIRE].

JHEP05(2020)092

[17] J.R. Ellis, K. Enqvist and D.V. Nanopoulos, *A Very Light Gravitino in a No Scale Model*, *Phys. Lett.* **147B** (1984) 99 [INSPIRE].

[18] J.R. Ellis, K. Enqvist and D.V. Nanopoulos, *Noncompact supergravity solves problems*, *Phys. Lett.* **151B** (1985) 357 [INSPIRE].

[19] A. Brignole, F. Feruglio and F. Zwirner, *Aspects of spontaneously broken $N = 1$ global supersymmetry in the presence of gauge interactions*, *Nucl. Phys.* **B 501** (1997) 332 [hep-ph/9703286] [INSPIRE].

[20] T. Gherghetta and A. Pomarol, *Bulk fields and supersymmetry in a slice of AdS*, *Nucl. Phys.* **B 586** (2000) 141 [hep-ph/0003129] [INSPIRE].

[21] T. Gherghetta and A. Pomarol, *A Warped supersymmetric standard model*, *Nucl. Phys.* **B 602** (2001) 3 [hep-ph/0012378] [INSPIRE].

[22] A. Brignole, J.A. Casas, J.R. Espinosa and I. Navarro, *Low scale supersymmetry breaking: Effective description, electroweak breaking and phenomenology*, *Nucl. Phys.* **B 666** (2003) 105 [hep-ph/0301121] [INSPIRE].

[23] I. Navarro, *Phenomenology of low scale supersymmetry breaking models*, *Mod. Phys. Lett.* **A 18** (2003) 2227 [hep-ph/0308196] [INSPIRE].

[24] I. Antoniadis, E. Dudas and D.M. Ghilencea, *Goldstino and sgoldstino in microscopic models and the constrained superfields formalism*, *Nucl. Phys.* **B 857** (2012) 65 [arXiv:1110.5939] [INSPIRE].

[25] E. Dudas, C. Petersson and P. Tziveloglou, *Low Scale Supersymmetry Breaking and its LHC Signatures*, *Nucl. Phys.* **B 870** (2013) 353 [arXiv:1211.5609] [INSPIRE].

[26] D.V. Volkov and V.A. Soroka, *Higgs Effect for Goldstone Particles with Spin 1/2*, *JETP Lett.* **18** (1973) 312 [INSPIRE].

[27] S. Deser and B. Zumino, *Broken Supersymmetry and Supergravity*, *Phys. Rev. Lett.* **38** (1977) 1433 [INSPIRE].

[28] E. Cremmer, B. Julia, J. Scherk, P. van Nieuwenhuizen, S. Ferrara and L. Girardello, *Super-Higgs effect in supergravity with general scalar interactions*, *Phys. Lett.* **79B** (1978) 231 [INSPIRE].

[29] E. Perazzi, G. Ridolfi and F. Zwirner, *Signatures of massive sgoldstinos at hadron colliders*, *Nucl. Phys.* **B 590** (2000) 287 [hep-ph/0005076] [INSPIRE].

[30] D.S. Gorbunov and A.V. Semenov, *CompHEP package with light gravitino and sgoldstinos*, hep-ph/0111291 [INSPIRE].

[31] D.V. Dyakonov, *The sgoldstino-Higgs sector interaction in the supersymmetric extension of the Standard Model* (in Russian), Bachelor GQT, MIPT (2018).

[32] S.P. Martin, *A Supersymmetry primer*, hep-ph/9709356 [INSPIRE].

[33] C. Petersson and A. Romagnoni, *The MSSM Higgs Sector with a Dynamical Goldstino Supermultiplet*, *JHEP* **02** (2012) 142 [arXiv:1111.3368] [INSPIRE].

[34] I. Antoniadis, E.M. Babalic and D.M. Ghilencea, *Naturalness in low-scale SUSY models and "non-linear" MSSM*, *Eur. Phys. J.* **C 74** (2014) 3050 [arXiv:1405.4314] [INSPIRE].

[35] M. Asano and R. Garani, *Sgoldstino search at the LHC*, arXiv:1701.00829 [INSPIRE].

[36] E. Perazzi, G. Ridolfi and F. Zwirner, *Signatures of massive sgoldstinos at e^+e^- colliders*, *Nucl. Phys.* **B 574** (2000) 3 [hep-ph/0001025] [INSPIRE].

JHEP05(2020)092

[37] D.S. Gorbunov and N.V. Krasnikov, *Prospects for sgoldstino search at the LHC*, *JHEP* **07** (2002) 043 [hep-ph/0203078] [INSPIRE].

[38] K.O. Astapov and S.V. Demidov, *Sgoldstino-Higgs mixing in models with low-scale supersymmetry breaking*, *JHEP* **01** (2015) 136 [arXiv:1411.6222] [INSPIRE].

[39] R. Ding et al., *Systematic Study of Diphoton Resonance at 750 GeV from Sgoldstino*, *Int. J. Mod. Phys.* **A 31** (2016) 1650151 [arXiv:1602.00977] [INSPIRE].

[40] S.V. Demidov and I.V. Sobolev, *Low scale supersymmetry at the LHC with jet and missing energy signature*, arXiv:1709.03830 [INSPIRE].

[41] M. Spira, *QCD effects in Higgs physics*, *Fortsch. Phys.* **46** (1998) 203 [hep-ph/9705337] [INSPIRE].

[42] J. Pumplin, D.R. Stump, J. Huston, H.L. Lai, P.M. Nadolsky and W.K. Tung, *New generation of parton distributions with uncertainties from global QCD analysis*, *JHEP* **07** (2002) 012 [hep-ph/0201195] [INSPIRE].

[43] C. Anastasiou et al., *CP-even scalar boson production via gluon fusion at the LHC*, *JHEP* **09** (2016) 037 [arXiv:1605.05761] [INSPIRE].

[44] G. Brooijmans et al., *Les Houches 2015: Physics at TeV colliders — new physics working group report*, in *9th Les Houches Workshop on Physics at TeV Colliders (PhysTeV 2015)*, Les Houches, France, 1–19 June 2015 (2016) [arXiv:1605.02684] [INSPIRE].

[45] R.V. Harlander, S. Liebler and H. Mantler, *SusHi Bento: Beyond NNLO and the heavy-top limit*, *Comput. Phys. Commun.* **212** (2017) 239 [arXiv:1605.03190] [INSPIRE].

[46] ATLAS collaboration, *Search for WW/WZ resonance production in $\ell\nu qq$ final states in pp collisions at $\sqrt{s} = 13$ TeV with the ATLAS detector*, *JHEP* **03** (2018) 042 [arXiv:1710.07235] [INSPIRE].

[47] ATLAS collaboration, *Search for heavy resonances decaying into WW in the $e\nu\mu\nu$ final state in pp collisions at $\sqrt{s} = 13$ TeV with the ATLAS detector*, *Eur. Phys. J.* **C 78** (2018) 24 [arXiv:1710.01123] [INSPIRE].

[48] ATLAS collaboration, *Searches for heavy ZZ and ZW resonances in the $\ell\ell qq$ and $\nu\nu qq$ final states in pp collisions at $\sqrt{s} = 13$ TeV with the ATLAS detector*, *JHEP* **03** (2018) 009 [arXiv:1708.09638] [INSPIRE].

[49] CMS collaboration, *Search for $Z\gamma$ resonances using leptonic and hadronic final states in proton-proton collisions at $\sqrt{s} = 13$ TeV*, *JHEP* **09** (2018) 148 [arXiv:1712.03143] [INSPIRE].

[50] ATLAS collaboration, *Searches for the $Z\gamma$ decay mode of the Higgs boson and for new high-mass resonances in pp collisions at $\sqrt{s} = 13$ TeV with the ATLAS detector*, *JHEP* **10** (2017) 112 [arXiv:1708.00212] [INSPIRE].

[51] ATLAS collaboration, *Search for new phenomena in high-mass diphoton final states using 37 fb^{-1} of proton-proton collisions collected at $\sqrt{s} = 13$ TeV with the ATLAS detector*, *Phys. Lett.* **B 775** (2017) 105 [arXiv:1707.04147] [INSPIRE].

[52] ATLAS collaboration, *Search for pair production of Higgs bosons in the $b\bar{b}b\bar{b}$ final state using proton-proton collisions at $\sqrt{s} = 13$ TeV with the ATLAS detector*, *JHEP* **01** (2019) 030 [arXiv:1804.06174] [INSPIRE].

[53] ATLAS collaboration, *Search for Higgs boson pair production in the $\gamma\gamma b\bar{b}$ final state with 13 TeV pp collision data collected by the ATLAS experiment*, *JHEP* **11** (2018) 040 [arXiv:1807.04873] [INSPIRE].

JHEP05(2020)092

[54] ATLAS collaboration, *Search for Higgs boson pair production in the $\gamma\gamma WW^*$ channel using pp collision data recorded at $\sqrt{s} = 13$ TeV with the ATLAS detector*, *Eur. Phys. J.* **C 78** (2018) 1007 [arXiv:1807.08567] [INSPIRE].

[55] ATLAS collaboration, *Search for Higgs boson pair production in the $b\bar{b}WW^*$ decay mode at $\sqrt{s} = 13$ TeV with the ATLAS detector*, *JHEP* **04** (2019) 092 [arXiv:1811.04671] [INSPIRE].

[56] CMS collaboration, *Combination of searches for Higgs boson pair production in proton-proton collisions at $\sqrt{s} = 13$ TeV*, *Phys. Rev. Lett.* **122** (2019) 121803 [arXiv:1811.09689] [INSPIRE].

[57] ATLAS collaboration, *Search for Higgs boson pair production in the $WW^{(*)}WW^{(*)}$ decay channel using ATLAS data recorded at $\sqrt{s} = 13$ TeV*, *JHEP* **05** (2019) 124 [arXiv:1811.11028] [INSPIRE].

[58] CMS collaboration, *Search for resonances decaying to a pair of Higgs bosons in the $b\bar{b}q\bar{q}'\ell\nu$ final state in proton-proton collisions at $\sqrt{s} = 13$ TeV*, *JHEP* **10** (2019) 125 [arXiv:1904.04193] [INSPIRE].

[59] J.S. Kim, S. Pokorski, K. Rolbiecki and K. Sakurai, *Gravitino vs Neutralino LSP at the LHC*, *JHEP* **09** (2019) 082 [arXiv:1905.05648] [INSPIRE].

[60] CMS collaboration, *Search for supersymmetry in final states with photons and missing transverse momentum in proton-proton collisions at* 13 TeV, *JHEP* **06** (2019) 143 [arXiv:1903.07070] [INSPIRE].

[61] CMS collaboration, *Search for supersymmetry in events with a photon, jets, b-jets and missing transverse momentum in proton-proton collisions at* 13 TeV, *Eur. Phys. J.* **C 79** (2019) 444 [arXiv:1901.06726] [INSPIRE].

[62] CMS collaboration, *Inclusive search for supersymmetry in pp collisions at $\sqrt{s} = 13$ TeV using razor variables and boosted object identification in zero and one lepton final states*, *JHEP* **03** (2019) 031 [arXiv:1812.06302] [INSPIRE].

[63] CMS collaboration, *Search for supersymmetry in events with a photon, a lepton and missing transverse momentum in proton-proton collisions at $\sqrt{s} = 13$ TeV*, *JHEP* **01** (2019) 154 [arXiv:1812.04066] [INSPIRE].

[64] ATLAS collaboration, *Search for supersymmetry in events with four or more leptons in $\sqrt{s} = 13$ TeV pp collisions with ATLAS*, *Phys. Rev.* **D 98** (2018) 032009 [arXiv:1804.03602] [INSPIRE].

[65] ATLAS collaboration, *Search for photonic signatures of gauge-mediated supersymmetry in* 13 TeV *pp collisions with the ATLAS detector*, *Phys. Rev.* **D 97** (2018) 092006 [arXiv:1802.03158] [INSPIRE].

JHEP05(2020)092